Heliyon 9 (2023) e13326

Contents lists available at ScienceDirect

Heliyon

journal homepage: www.cell.com/heliyon

Research article

Extreme rainfall characterisation under climate change and rapid population growth in the city of Niamey, Niger

Issa Garba, Zakari Seybou Abdourahamane *

Agrhymet Regional Centre, Niamey, Niger

A R T I C L E I N F O

Keywords:
Augmented Dickey Fuller test
Climate projection
Extreme rainfall
Generalised pareto distribution
Mann-Kendall test
Peak over threshold
Pluvial flood

A B S T R A C T

Since recent years, the Sahel semiarid region has experienced devastating floods—causing significant losses and damages. The present paper attempts to characterise extreme rainfalls responsible for pluvial floods in the city of Niamey, in Niger, under climate change and rapid population growth. Past damaging rainfall records spanning 1992–2015 were used to estimate the optimal temporal scale and to define a threshold for extreme rainfall. The characteristics of extreme rainfalls were then assessed under stationary and non-stationary conditions using peaks over threshold (POT) with the generalised pareto distribution (GDP). In the non-stationary POT, population data was used as threshold covariate whereas air temperature was used as scale parameter covariate. A suitable temporal scale of 3 h was found, whereas the threshold depth was 28.71 mm under stationary conditions and between 21 and 27 mm for the time dependent threshold. The analysis of the extreme rainfall series revealed no significant trend neither in the magnitude nor in the frequency. The influence of air temperature in the characterization of extreme rainfall were less compared to rapid urbanisation, represented herein by population growth. By 2040, 3-hourly rainfall depths of 20 mm could be considered as extreme rainfall.

1. Introduction

Since recent years, floods in the West African Sahel (WAS) have become a significant threat to human life, economy and environment. The causes behind the increase of urban flood, in terms of frequency and intensity, are multifaceted—varying from the intensification of heavy rainfall events to the modification of the geomorphological characteristics of urban catchments. In the Sahel region, heavy rainfalls have been associated with large scale climate indices. Paeth et al. [1] attributed the Sahelian 2007 floods to heavy rainfall induced by largescale climate phenomena, such as la Niña event in the tropical pacific, anomalous heating in the tropical Atlantic and strong African easterly waves. Mouhamed et al. [2] sustained that during the 2000s extreme rainfalls have increased in frequency over the WAS, leading to the occurrence of more floods at about 8–12 events per year while it was only 2 events per year during the drought period. These findings were sustained by Ref. [3] who emphasized the positive trend in flood frequencies and intensities of the Sirba river, the main tributary of the inner Niger basin.

The causes of flood are difficult to determine since the physical characteristics of catchments such as the topography, the geomorphology and the land cover play an important role in the rainfall-runoff process. Thus, the cause of floods in WAS cannot be resumed to only heavy rainfall intensifications. Several studies have shown that rainfall-induced floods in the WAS region are not unprecedented, and have return periods less than 50 years [4,5]. Therefore, the degradation of the physical characteristics of WAS

* Corresponding author.
E-mail address: azakari.seybou@yahoo.fr (Z.S. Abdourahamane).

https://doi.org/10.1016/j.heliyon.2023.e13326
Received 9 August 2022; Received in revised form 24 January 2023; Accepted 26 January 2023
Available online 29 January 2023

catchments have played an important role in the occurrence of recent floods. Other studies have attributed the floods to land use land cover changes [6–8], the negative consequences of the Sahelian prolonged drought (loss of vegetation and modification of soil properties) [9], the extension of crop lands [10], the rapid urbanization and climate change [11].

From the above-mentioned studies, both climate change and direct anthropogenic activities have contributed to the intensification of floods in the WAS. Climate change, through the increase of the global temperature, is modifying the rainfall regime of many regions of the word. It is worth mentioning that rainfalls in the WAS mostly stem from mesoscale convective systems [12] which contribute to most of the extreme rainfall events [13]. The amount and occurrence of extreme rainfall produced through convective systems is related to temperature increase under many factors [14]; thus, is impacted by global warming. On the other hand, it is well-known that unsustainable use of land leads to an extension of impervious areas which in turns increases runoff amounts.

Urbanization, driven by population growth, has one of the most important anthropogenic influences on climate [15]. It is an important driver of ecosystem degradation and the disruption of the main ecosystem functions as found by Ref. [16] in Ethiopia. Yan et al. [17] estimated flood hazard under non-stationarity assumption using rainfall and population as covariates in two rivers basins of China, and found that both climate change and increased anthropogenic activities are responsible of the variability in flood occurrence.

Niger is the WAS country having the highest demographic growth with 3.9% per year [18]. A direct consequence of the rapid population growth is the urban sprawl in the country's main cities. These cities are characterised by a lack of appropriate drainage system due to limited financial resources and urban planning. While the implementation of pragmatic actions to cope with flood is still waiting, people in Niger are suffering from its disastrous consequences. For instance, in 2017, 56 people died due to heavy rains that caused floods [19]. Additionally, studies investigating the hydroclimatic conditions that trigger urban floods in the country are scarce and the behaviour of the extreme rainfalls remains unexplored.

As the casualties and economic losses are rapidly increasing, especially in urban areas, a characterization of extreme rainfall under climate change and land-use/land-cover (LULC) changes is necessary to improve the prediction of rainfalls that cause disaster. A grasp of the characteristics (depth, duration, intensity, trend, return levels) of the extreme rainfalls events as well as the contribution of LULC changes to floods intensification under present and future conditions is necessary. However, the concept of extreme rainfall varies from one region to another or even differs according to the seasons or from rural to urban areas. The climate change impacts on the spatiotemporal rainfall variability over many regions is making more challenging the definition of extreme rainfall. An objective-oriented definition of extreme rainfall, such as flood analysis, land slide or urban infrastructure design, may result more useful for decision makers and stakeholders.

Among the methods used for extreme rainfall analysis is Peaks Over-Threshold [20] which has been used to model extreme rainfall under stationary and non-stationary conditions over many regions [21–23]. Chamani, Monkam [24] used stationary POT to estimate the return levels and return period of extreme rainfall in the Sahel region, The POT analysis begins with the definition of a threshold value above which extreme rainfall is defined. Several methods exist for the selection of the threshold value, such as graphical approaches, methods based on the goodness of fit or simply objective-oriented threshold selection. The residual life plot and the threshold stability plots are the most commonly used graphical approaches [25,26]. However, these methods may result inefficient in presence of a large amount of data or in cases where multiple threshold values are required [26]. The goodness of fit approach consists of checking how the empirical distribution of the threshold exceedances fit the generalised pareto distribution (GPD) by using for example the Kolmogorov-Smirnov test or the Anderson–Darling test [25]. In some cases, the threshold is fixed to a certain value such as the 95th percentile [27] or the 99th percentile [28]. Other methods are based on bias estimation using, for example, the bootstrap analysis [29] or by fixing the mean number at which the threshold is exceeded within a determined interval of period [21].

In the WAS context, characterised by a high socio-economic and environmental vulnerability to climate change and under the current urbanization conditions, a threshold selection method that account for the local physical characteristics and the socioeconomic conditions may result more suitable for flood and rainfall-related disaster management. Additionally, the duration of rainfall events, mainly when originating from convective systems, is affected by global warning. Moreover, the hydrological process in urban areas is characterised by a high spatiotemporal variability. Therefore, the choice of an appropriate temporal scale is crucial for extreme rainfall modelling.

The present paper attempts to characterise the extreme rainfall responsible for pluvial flood in the city of Niamey in terms of duration, depth, intensity, trend, return level and their behaviour under temperature increase and population growth. Therefore, the paper aims to (i) determine the appropriate temporal resolution for extreme rainfall analysis using historical rainfall records; (ii) define a threshold depth above which extreme rainfalls are defined; (iii) determine the behaviour of the extreme rainfalls in terms of trends and return levels using a stationary threshold (POT) based on Generalised Pareto Distribution (GDP) and a non-stationary POT with population data as threshold covariate and air temperature as the GPD scale parameter's covariate; and finally, (iv) evaluate the future extreme rainfall characteristics using projected air temperature and projected population data.

The use of the air temperature directly reflects the effect of global warming on extreme rainfall patterns, whereas population data is a good indicator of the human stress on the geomorphological characteristics of urban catchments, including land use land cover changes and urban sprawl.

2. Material and methods

2.1. Study area

Located in the south-west of the country specifically along the banks of the Niger River (Fig. 1), Niamey is the capital city of Niger since 1926. Currently, it is the most populated city of the country with more than 1.3 million inhabitants [18]. The city extends over 240 km^2 divided into five administrative districts—four located in the left bank and one in the right bank of the Niger river. The altitudes throughout the city vary between 180 and 250 m and the mean annual rainfall is about 550 mm [30]. Monthly temperatures oscillate between 32.5 °C in January, the coolest month, and 40.9 °C in April, the warmest month.

The city of Niamey is mainly characterised by a rapid population growth which leads to an increase of informal settlements including in flood prone areas such as water courses or tributaries of the Niger river. Urban drainage networks in the city are scarce. Currently, both fluvial floods—over bank flow of the river Niger—and pluvial floods constitute a threat to the population of Niamey.

2.2. Data description

2.2.1. Rainfall data

In the city of Niamey, sub-daily rainfall records were scarce until 1990 when the African Monsoon Multidisciplinary Analysis-Coupling the Tropical Atmosphere and the Hydrological Cycle project, with its acronym in French AMMA-CATH (Analyse Multi-disciplinare de la Mousson Africaine - Couplage de l'Atmosphere Tropicale et du Cycle Hydrologique) started its first measurements. In the present study the 5-min rainfall record of Jun-July-August-September (JJAS) at four rain gauges were used. Three of these rain gages are located in the city of Niamey and one in its peripheries (Fig. 1). These data were retrieved from the AMMA-CATH database [31], and span the period 1992–2015. The details of the considered rain gauges and the recorded storm events during the study period are given in Table 1. The missing rainfall records at all the stations is less than 5% and were discarded for the analysis.

2.2.2. Air temperature data

To integrate the effect of climate change in the extreme rainfall characterization over the city of Niamey, air temperature data were used as covariate in a nonstationary peak over threshold model. For this purpose, the NCEP/NCAR Reanalysis 1 [15] gridded (2.5° × 2.5°) monthly air temperature data at 2 m level were used as a GDP scale parameter's covariate. The use of air temperature in the characterization of extreme rainfall reflects the influence of temperature increase in the extreme rainfall magnitudes and frequencies.

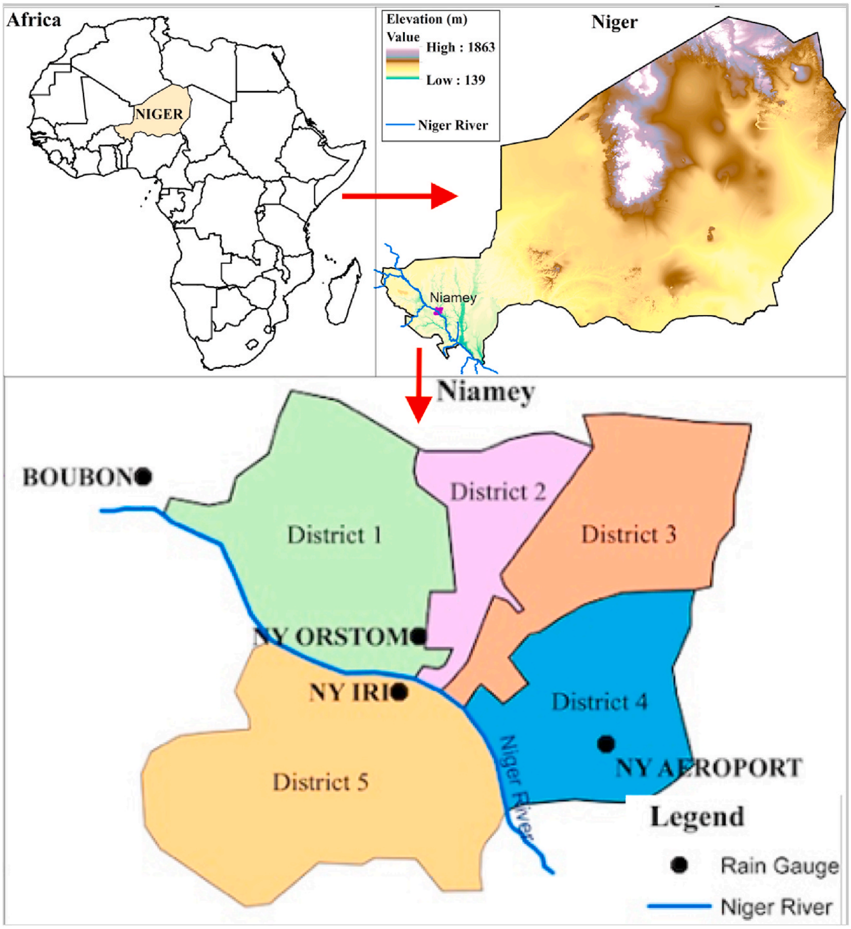

Fig. 1. Study area.

Table 1
Detail of the rain gauges and recorded rainfall events between 1992 and 2015.

Station name	Regional Code	Lon. (°)	Lat. (°)	Alt. (m)	missing data (%)	Nr. of events ≥ 1 mm	Mean depth (mm)	Mean duration (h)	Mean intensity (mm/h)
Ny Aero	1321209400	2.183	13.479	223.00	3.63	805	13.24	1.75	11.83
Ny Orstom	1321207000	2.094	13.530	223.00	0.20	826	14.01	1.77	10.33
Ny Iri	1321208300	2.085	13.504	187.00	3.36	797	14.28	1.82	8.42
Boubon	1321208500	1.964	13.606	211.00	4.64	758	14.7	1.73	8.75

Note: The number of events, mean depth, mean duration and mean intensity are for the rainfall events with depth greater or equal to 1 mm.

2.2.3. Historical flood events

The rainfall depth, duration and intensity of 30 storm events during which pluvial floods or catastrophes have occurred were collected for the period 1992–2015. The date of occurrence of these floods were retrieved from the ministry of humanitarian action and disasters management, the Emergency Events Database EM-DAT [32], the NatCatService (http://www.munichre.com/touch/naturalhazards); the Humanitarian Data Exchange (HDX, https://data.humdata.org/) of the United Nations Office for the Coordination of Humanitarian Affairs (OCHA), the OCHA Global Active Archive of Large Flood Events, the famine early warning system (http://fews.net/) of the USAID and the UN Reliefweb (https://reliefweb.int/). The storms responsible for these reported floods were identified and their characteristics were assessed. The date of occurrence of the 30 pluvial floods or rainfall-related disaster are presented in Table 2.

2.2.4. Demographic data of Niamey

The demographic growth rate of Niger is one of the highest of the world. One of the main consequences of this rapid population growth is the increase of urban sprawl in the country's main cities. As urban sprawl is one of the main factors that increase the occurrence of urban pluvial flood, demographic data of the city of Niamey were used in the characterisation of rainfall-triggering flood. The demographic data were retrieved from the national statistics institute of Niger [33]. Fig. 2 shows the evolution of the population of Niamey between 1978 and 2018.

The projected population data for the period 2020–2050 were computed based on the demographic growth rate of the city of Niamey estimated in 2018 at 3.19% per year [32].

2.2.5. Projected air temperature

The effect of temperature increase on future extreme rainfall was analyzed using projected monthly air temperature data for the period 2020–2050. The projected air temperature data from four Earth System Models (ESM) of CMIP5 (Coupled Model Intercomparison Project Phase 5) under the RCP8.5 concentration scenario were considered. The projected data were interpolated at the 0.5° squared grid of the city of Niamey. Details of the ESM are presented in Table 3.

2.3. Methods

2.3.1. Selection of the rainfall temporal resolution

Several studies have addressed the selection of an optimal temporal resolution for urban hydrological applications. In the present paper, the finest temporal resolution of the rainfall records which is available in the study area (5-min) was used to characterise (depth, duration and intensity) the considered 30 storms during which pluvial floods were reported (Table 2). Due to the high spatial variability of the rainfall pattern over the city of Niamey, the recorded rainfall amounts during a reported flood may differ significantly from one station to another. To avoid considering rainfall amounts recorded far from flooded areas as flood triggering rainfalls, observations less than the average (depth and duration) of the registered rainfall events between 1992 and 2015 were discarded.

A rainfall-triggering flood (*R_flood*) is thus defined at each station as a rainfall recorded during a reported flood in the city of Niamey with an intensity greater than the long-term average of 1992–2015 shown in Table 1 ($I_{R\_flood} > I_{R\_1992-2015_{average}}$).

The average rainfall-triggering flood duration at each gauge $D_{R\_flood_{gauge}}$ was computed as the arithmetic mean of the duration of all

Table 2
Considered flood events.

Event Number	1	2	3	4	5	6
Date of Occurrence	July 27, 1992	July 31, 1992	13/08-1994	August 22, 1994	August 23, 1995	July 23, 1996
Event Number	7	8	9	10	11	12
Date of Occurrence	June 30, 1998	August 28, 1998	July 25, 1999	June 28, 2001	June 14, 2002	July 31, 2002
Event Number	13	14	15	16	17	18
Date of Occurrence	7/6/05	20-09-2005	24-08-2006	4/8/07	7/11/08	16-08-2009
Event Number	19	20	21	22	23	24
Date of Occurrence	9/2/09	11/7/10	5/8/11	19/08/12	21/08/12	6/8/13
Event Number	25	26	27	28	29	30
Date of Occurrence	31-07-2014	22/08/14	24-09-2014	12/7/15	19-07-2015	17/08/15

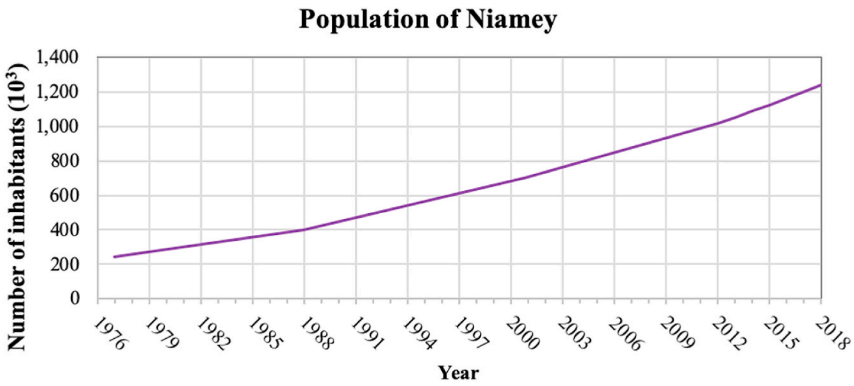

Fig. 2. Evolution of the population of Niamey between 1976 and 2018.

Table 3
Detail of the Earth system models.

Model Name	Institution
IPSL-CM5A-LR	Institut Pierre Simon Laplace, Paris, France
MIROC-ESM-CHEM	Japan Agency for Marine-Earth Science and Technology, Kanagawa, Japan
MPI-ESM	Max Planck Institute for Meteorology, Hamburg, Germany
GFDL-ESM2M	NOAA Geophysical Fluid Dynamics Laboratory, Princeton New Jersey, USA

the catastrophic storm events registered at this gauge. The temporal resolution for the extreme rainfall analysis in the city of Niamey was chosen as the mean $D_{R\_flood_{gauge}}$ of the four rain gauges using Equation (1):

$$\Delta t_r = \frac{1}{N}\sum_{i=1}^{N} D_{R\_flood_{gauge(i)}} \tag{1}$$

here N is equal to 4 which is the number of rain gauges and i is an integer varying between 1 and N.

The average duration at all the station Δt_r resulted equal to 2.62 h, which was rounded to 3 h. Therefore, a Δt_r equal to 3 h was selected as the optimal temporal resolution for the extreme rainfall analysis over Niamey.

2.3.2. Behaviour of the 3-hourly rainfall: trend and stationarity

Once the optimal temporal resolution of the rainfall data was determined, the next step consisted of looking for trend and stationarity in the rainfall series. Two methods were applied for the trend analysis—the classical Mann-Kendall (MK) test [34] and the trend free pre-whitening MK (TFPMK) test [35] depending on the absence or presence of serial correlation in the data, respectively, and following [36]. The serial correlation was assessed by plotting the autocorrelation function (ACF). Finally, the Augmented Dickey-Fuller (ADF) test [37,38] was used to assess the presence of stationarity. The ADF test assumes under the null hypothesis that a time series has a unit root, thus is non-stationary. The alternative hypothesis implies that the series are stationary. More details on the ADF test can be found in Refs. [37,38].

2.3.3. Extreme rainfall analysis: peaks over threshold

In the POT analysis, the identification of extreme values of a time series $x_1, x_2, x_3, \ldots, x_n$ begins with the selection of the threshold u, above which the set of extreme events are defined as $\{x_i > u\}$. The threshold exceedances are then derived by subtracting the threshold value from the extreme values $x_i - u, with\ i = 1, \ldots k$; k being the number of threshold exceedance. The exceedances are then fitted to a probability distribution function. Coles [20] suggests considering the excess distribution as independent random variable that follows approximately a Generalised Pareto distribution (GPD). On the other hand, the rate of occurrence of these exceedances is considered to follow a Poisson distribution with an average rate of occurrence λ in a certain time interval. Therefore, the GPD was used to model the rainfall exceedances, while the return levels of the exceedance were modelled using the GPD-Poisson distribution following [20].

2.3.4. Estimation of the distribution parameters

The threshold of the stationary POT is determined based on the intensities of the historic rainfalls that have triggered pluvial flood in the city of Niamey. The minimum rainfall intensity of the pluvial flood-triggering rainfall events was retained as the threshold intensity value (I_u) above which extreme rainfall is defined. The rainfall threshold depth u is therefore computed using Equation (2):

$$u = \mu = \Delta t_r * I_u \tag{2}$$

here, $\Delta t_r = 3\,h$ is the temporal resolution and $I_u = \min\,(I_{R\_flood})$ is the threshold intensity.

To assess the uncertainty that may generate this approach, the 95th and 99th percentiles of the 3-hourly rainfall depth greater or equal to 1 mm were used as thresholds in two different POT models. The results of the POT for the three thresholds—the threshold based on the flood triggering rainfall hereinafter referred as U_flood, the 95th percentile threshold (U_95th) and the 99th percentile threshold (U_99th)—were then compared to each other using the GPD parameters error estimates and the quantile-quantile (Q-Q) plots.

As for the nonstationary POT model, the threshold is computed as a function of the evolution of the population and the scale parameter was computed as a function of the monthly air temperature at 2 m level, whereas the shape parameter was maintained constant. Therefore, it was possible to assess the behaviour of future extreme rainfall using projected temperature and population data.

The fitting of the threshold exceedance to the GPD was performed in R statistical software [39] using the "ismev" package [40].

3. Results

3.1. Trend and stationarity analysis

Prior to the trend test, a serial correlation analysis was performed on the 3-hourly rainfall series using autocorrelation functions (ACF) plots. The selection of the trend method depends on the outcome of the ACF plots which shows either the series are serially correlated or independent. The ACF plots of the rainfall series displayed in Fig. 3 revealed a significant lag-1 autocorrelation at the 95% confidence level at all the four stations. The TFPWMK test was then applied to detect trend in the 3-hourly rainfall series.

The result of the TFPWMK analysis is presented in Table 4. To reject the null hypothesis (at $p = 5\%$) which assumes that the series have no trend, the test statistics Z-value must fall outside the confidence interval which is [−1.96, 1.96], otherwise the null hypothesis is accepted. From Table 4, the series of the four rain gauges have no significant trend over the period 1992–2015 as the TFPWMK failed to reject the null hypothesis.

To assess the stationarity of the 3-hourly rainfall series the ADF test was applied. The output of the ADF test is presented in Table 5. From this table, it can be seen that the null hypothesis was rejected at the 1% significance level; hence, the 3-hourly rainfall series are stationary during the study period.

3.2. Stationary threshold and construction of the extreme rainfall series

After determining the behaviour of the 3-hourly rainfall series, the fixed threshold depth above which extreme precipitation is defined in the city of Niamey was computed using Eq. (2), and the series of the extreme rainfall were formed. The threshold intensity and depth at each of the considered rain gauges are described in Table 6.

The results of the trend analysis using the TFPMK test are presented in (Table 7). These results revealed no significant trend at the four rain gauges.

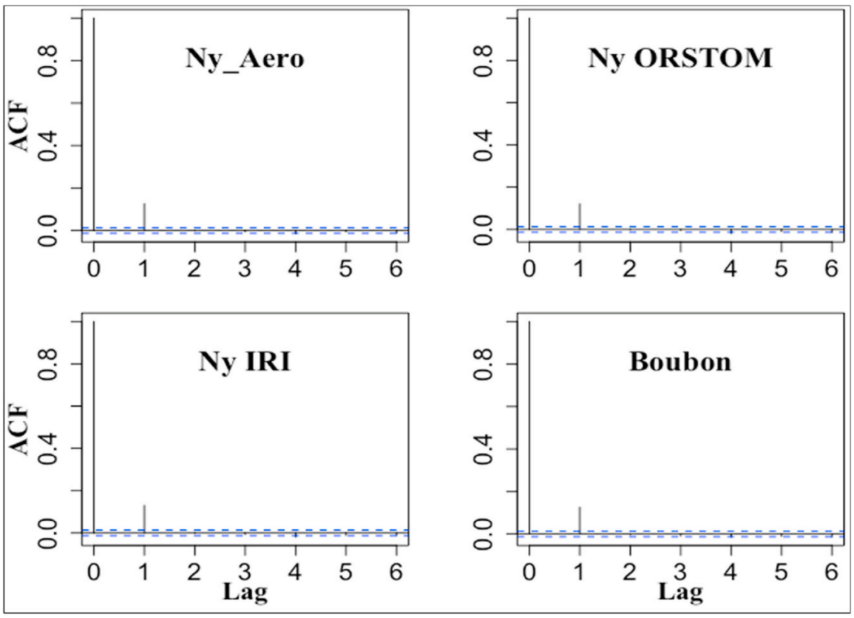

Fig. 3. ACF of the 3-hourly rainfall series at the considered stations.

Table 4
Results of the TFPWMK test for the 3-hourly rainfall series.

Station	Z-Value	Sen's Slope	Old Sen's Slope	P-value	S	Var(S)	Tau
Niamey_Aero	−0.084	0.0001	0.000	0.933	−5.05E + 04	3.66E + 11	−1.98E − 04
Ny IRI	0.514	0.0001	0.000	0.608	3.19E + 05	3.85E + 11	1.24E − 03
Ny ORSTOM	0.542	0.0001	0.000	0.588	3.45E + 05	4.05E + 11	1.26E − 03
Boubon	0.639	0.0001	0.000	0.523	3.75E + 05	3.44E + 11	1.50E − 03

Table 5
Results of the stationarity test of the 3-hourly rainfall series.

Station	Dickey-Fuller	Lag order	p-value	Inference
Ny Aero	−29.833	23	0.01	Stationary
Ny ORSTOM	−29.999	23	0.01	Stationary
Ny IRI	−29.770	23	0.01	Stationary
Boubon	−29.350	23	0.01	Stationary

3.3. Stationary POT analysis

In the stationary POT analysis, all the three GPD parameters are considered time-invariant. The estimated GPD parameters and errors estimates for each of the three thresholds (U_flood, U_95th percentile and U_99th percentile) are presented in Table 8 and the Q-Q plots are shown in Fig. 4, Fig. 5, and Fig. 6.

Table 8 shows that the threshold based on the rainfall-induced flood (U_flood) have the lowest standard error estimates of the GPD parameters, proving that it fits better the GPD.

Since the threshold computed using the minimum depth of the rainfall-triggering floods provides the best stationary GPD fitting, it was used to compute the stationary return levels. The computed return levels are plotted in Fig. 7.

The computed return levels at Ny Aero and NY ORSTOM are similar due to the high correlation that exist between their rainfall series. The ever recorded highest three-hourly rainfall depth is 112.15 mm, and has a return period of 63 years. The number of threshold exceedance per year is shown in Fig. 8. From this figure, the year 1998 was exceptional as it has the highest number of extreme rainfalls. Additionally, Fig. 8 reveals a slight decline in the number of extreme rainfalls per year between 1992 and 2015.

3.4. Non-stationary POT

Population data of Niamey and air temperature data at 2 m level between 1992 and 2015 were used as covariates in the non-stationary POT analysis. The regression coefficients of the covariate dependent location $\{\mu_0, \mu_1\}$ and covariate dependent scale $\{\sigma_0, \sigma_1\}$ parameters, respectively, are presented in Table 9.

The residual Q-Q plots of the non-stationary GPD fitting for the four rain gauges is shown in Fig. 9 and the 10, 20, 50 and 100 years non-stationary return levels as well as the time-dependent threshold are shown in Fig. 10.

The Q-Q plot shows that the time dependent location and scale parameter using population data and air temperature as covariates provide a suitable GDP fitting of the threshold exceedances.

3.5. Future extreme rainfall analysis

To choose the best model for projected air temperature data, a correlation analysis was carried out between observed air temperature of the NCEP/NCAR Reanalysis 1 and each of the considered ESM data of the CMIP5. The MPI-ESM model exhibited the highest correlation with a Pearson R = 0.91. Therefore, the MPI-ESM projected air temperature data was used to compute the scale parameter of the GPD for the period 2020–2050. Future non-stationary rainfall thresholds were computed using projected population data. The projected population data were computed using the demographic growth rate of the 2018 general census. The time dependent threshold and scale parameters enabled the computation of the return levels for the period 2020–2050. The projected return levels are

Table 6
Threshold-based rainfall-triggering flood and extreme rainfall events.

Name	I_U (mm/h)	U_flood (mm)	POT series length	Number of extreme events per month				Events between 6 p.m. and 6 a.m.
				Jun.	Jul.	Aug.	Sep.	
Ny Aero	9.28	27.84	76	9	25	35	7	65.79%
Ny Orstom	8.29	27	97	15	32	39	11	73.20%
Ny Iri	8.07	30	79	11	27	32	9	72.15%
Boubon	8.9	30	72	9	19	33	11	79.17%

Note: I_U is the threshold intensity and U_flood is the threshold depth.

Table 7
Results of the TFPWMK test of the extreme rainfall series.

Station	Z-Value	Sen's slope	S	Var(S)	P-value	Tau
Niamey_Aero	0.284	0.001	63	47791.67	0.77	0.02
Ny ORSTOM	−0.611	−0.015	−194.00	99813.33	0.54	−0.04
Ny IRI	−1.50	−0.055	−349.00	53720.33	0.13	−0.12
Boubon	−0.12	−0.007	−25.00	40588.33	0.90	−0.01

Table 8
Thresholds and standard error estimates.

Station name	Threshold (mm)			standard error estimates					
	U_flood	U_95th	U_99th	U_flood		U_95th		U_99th	
				Scale	Shape	Scale	Shape	Scale	Shape
Niamey_Aero	27.84	31.54	46.85	**1.798**	**0.124**	2.281	0.132	11.649	0.400
Ny ORSTOM	27	32.309	47.51	**1.213**	**0.102**	1.863	0.155	7.648	0.461
Ny IRI	30	32.82	51.79	**1.307**	**0.091**	1.963	0.220	17.441	0.442
Boubon	30	35.112	53.91	**2.428**	**0.111**	3.056	0.135	6.196	0.484

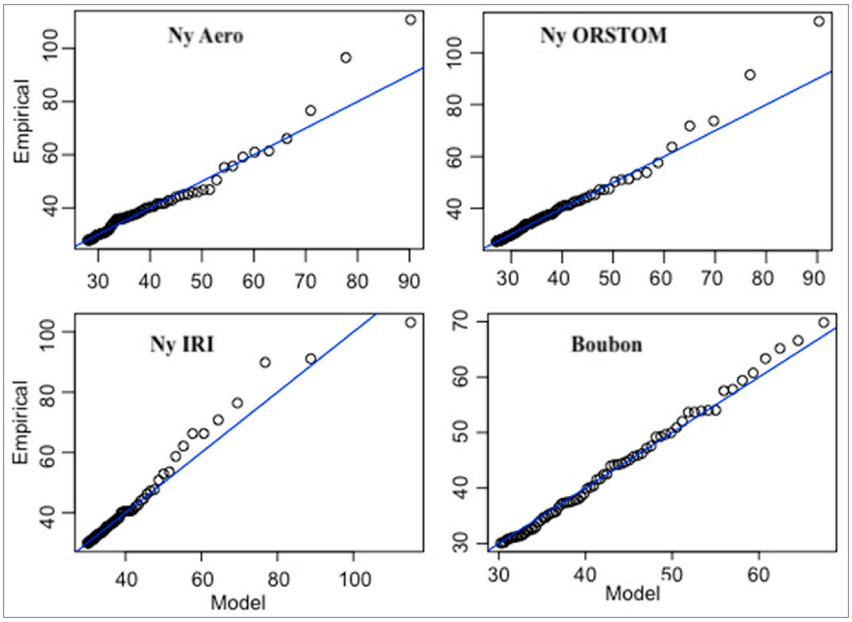

Fig. 4. Q-Q plots of the GPD model using the flood triggering based-threshold at the four stations.

presented in Fig. 12.

Fig. 12 shows that a decrease in the rainfall depth for each return level is expected for the period 2020–2050 at all the four rain gauges. The same figure shows that the threshold depth will decrease. Therefore, the number of damaging rainfall events will surge, making the city more vulnerable to extreme rainfall. By the late 2040 rainfall amount even less than 20 mm for a duration of 3 h will be expected to be damaging unless appropriate drainage systems are constructed, and a sustainable urban planning is adopted.

4. Discussion

The trend result in this paper corroborates the findings of [5] from which the rainfall indices on a daily basis do not show a significant trend in the Sahelian city of Ouagadougou (Burkina Faso). Moreover, the reliability of the ADF test depends on the choice of a suitable lag order, as different lag orders can yield different results for the same data. In general, when the lag order is low, serial correlation bias the test—in such a case the test tends to reject the null hypothesis (stationarity) and high lag-orders fail to reject the null hypothesis (non-stationarity). The optimal lag order was therefore selected based on the Akaike Information Criterion (AIC) [41]. The lowest AIC corresponding to the optimal lag order.

By considering the arithmetic mean of the depth thresholds of the four rain gauges, the extreme rainfall definition can be

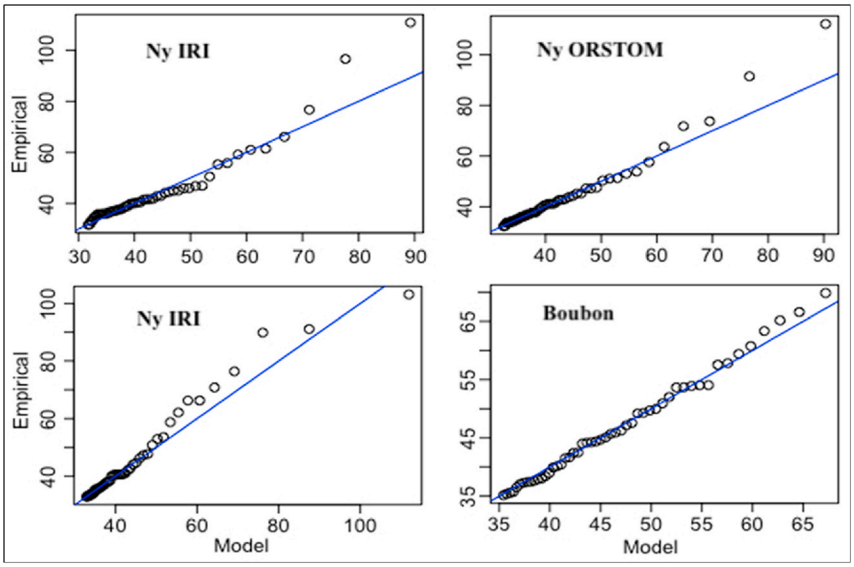

Fig. 5. Q-Q plots of the GPD model using the 95th percentile threshold at the four stations.

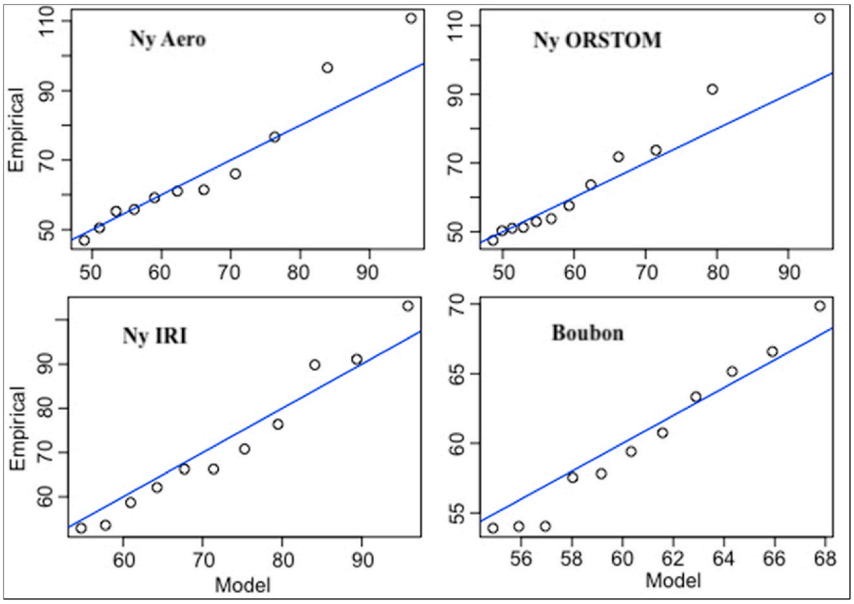

Fig. 6. Q-Q plots of the GPD model using the 99th percentile as threshold at the four stations.

generalised to the entire city of Niamey as any storm event recording a depth greater than 28.71 mm for a duration less than or equal to 3 h. Hence, an areal average of 81 extreme rainfall events occurred during 1992–2015, corresponding approximately to three events per year (JJAS). August is the month with more extremes followed by July, and around three-quarter of the extreme events occurred between 6 p.m. and 6 a.m. Also, the frequency distribution revealed that most of these extremes occurred during 12 a.m.–3 a.m. and 3 a.m.–6 a.m. The rainfall event with the highest ever recorded depth for a duration of 3 h or less was registered at Ny ORSTOM station with a depth of 112.15 mm on August 1st, 1998, between 12 a.m. and 3 a.m.

Additionally, the trend analysis of the extreme rainfall series revealed no significant trend at the 5% significance level. From the ADF test, only the extreme rainfall series at Ny IRI rain gauge is non-stationarity.

The superiority of the U_flood POT model is reflected on the Q-Q plots, confirming its outperformance over the 95th percentile and 99th percentiles thresholds based models. Additionally, the use of the 99th percentiles as threshold generates a small number of threshold exceedances—indicating its inappropriateness as threshold since it is too high and may fail to identify devastating rainfalls in the study area. Despite of having parameters error estimates greater than the U_flood, the U_95th percentile threshold provides a GPD

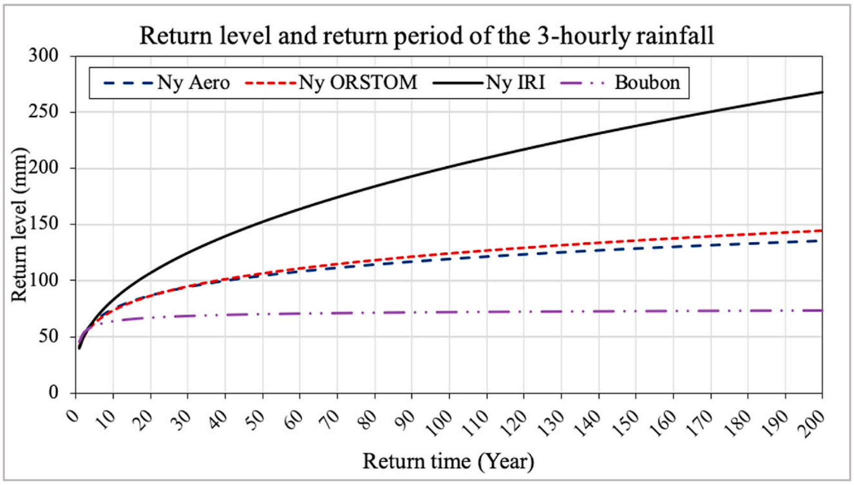

Fig. 7. Return levels and return periods using the stationary POT model.

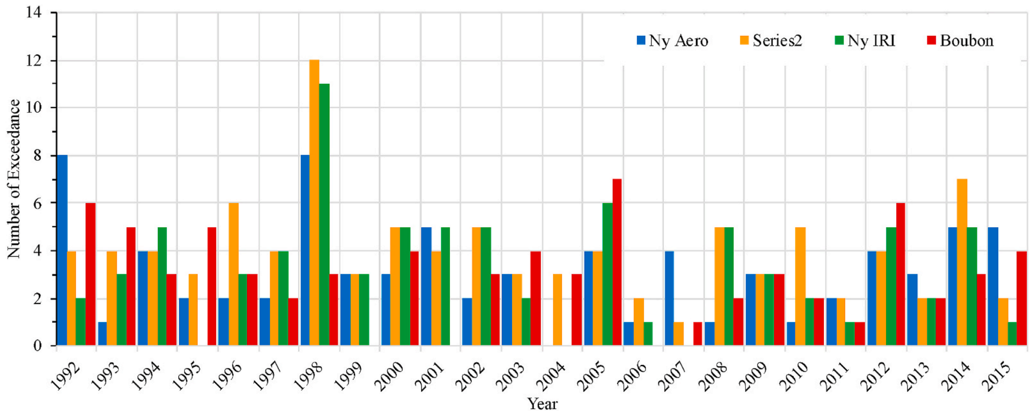

Fig. 8. Number of extreme rainfall events per year using the stationary POT.

Table 9
Coefficients of the non-stationary location and scale parameters.

Station	μ_0	μ_1	σ_0	σ_1
Ny Aero	27.84	−2.5E − 06	11.8589	−0.0312
Ny ORSTOM	27	−2.5E − 06	2.6604	−0.0015
Ny IRI	30	−3E − 06	0.7253	0.0043
Boubon	30	−3E − 06	8.8713	−0.0200

fitting suitable as can be seen in the Q-Q plots of Fig. 5. Its use as threshold is more reasonable than the 99th; however, performs less than the U_flood which may result more appropriate for an operational extreme rainfall analysis.

The computed return levels show that extreme rainfall as defined in this paper using the stationary threshold can occur from July to September. In terms of extreme value theory and in some analyses, an event with a return period less than a year may be discarded as extreme events. Nevertheless, the concept of extreme rainfall adopted in this paper aims to identify and characterise the rainfall events responsible for pluvial flood.

The time dependent threshold and the return levels (Fig. 10) show a slight downward trend at all the four rain gauges. This can be explained by the negative correlation between the threshold and the evolution of the population data over time. As the population increase in the city of Niamey, the urban sprawl spreads leading to an increase of the ratio of impervious areas which in turn augments the runoff amount.

The number of threshold exceedance per year using the non-stationary POT displayed in Fig. 11 shows that the number of extremes using the non-stationary POT model is higher than the ones of the stationary model due to the decreasing threshold depth over time. However, the number of exceedances per year for the non-stationary POT does not exhibit a significant trend despite the decreasing

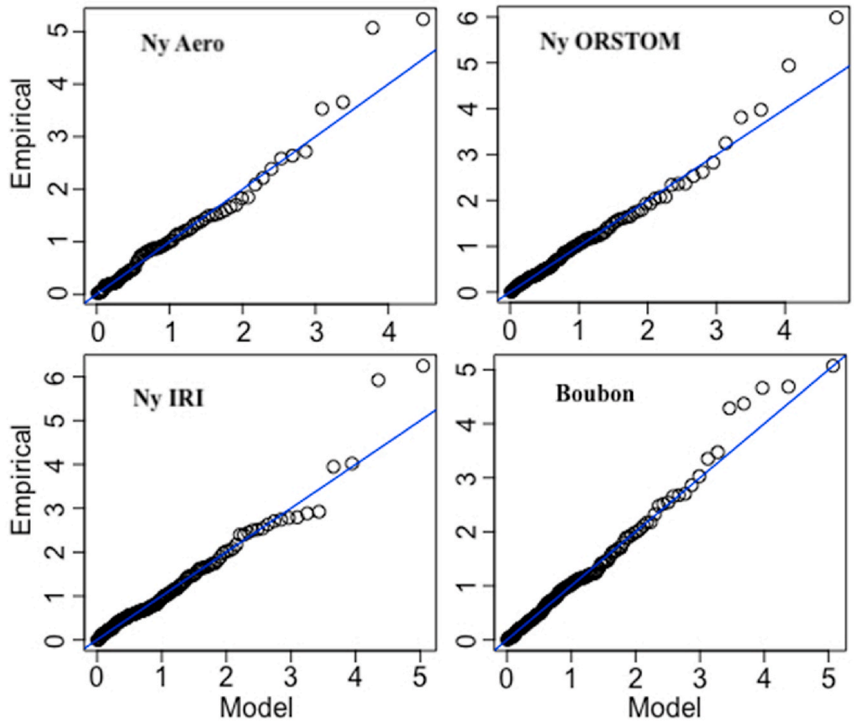

Fig. 9. Residual quantile plot of the nonstationary GPD at the four stations.

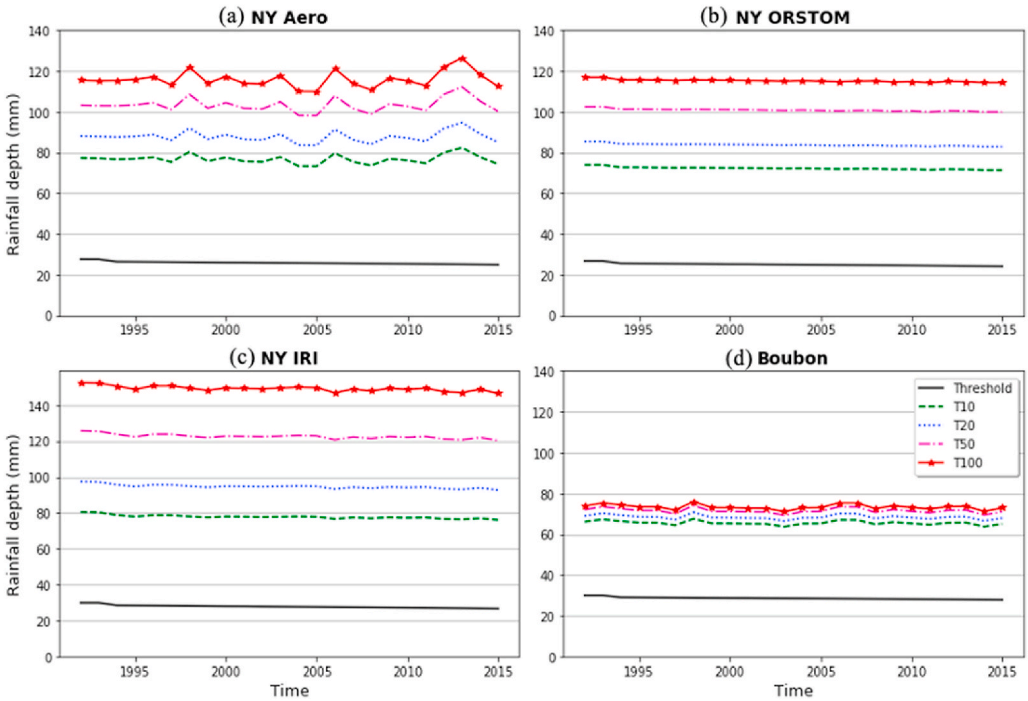

Fig. 10. Threshold and return levels of the nonstationary POT at Ny-Aero (a), Ny ORSTOM (b), Ny IRI (c) and Boubon (b) stations. The legend all the graphs is in panel (d).

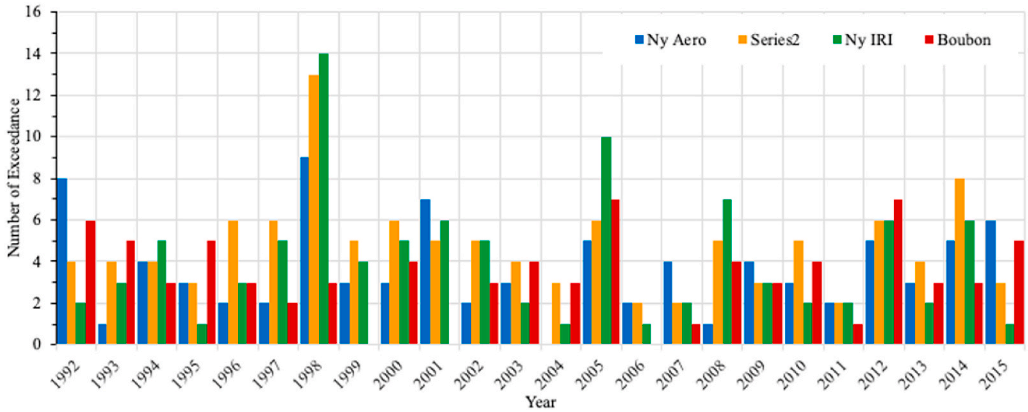

Fig. 11. Number of threshold exceedances per year using the non-stationary POT.

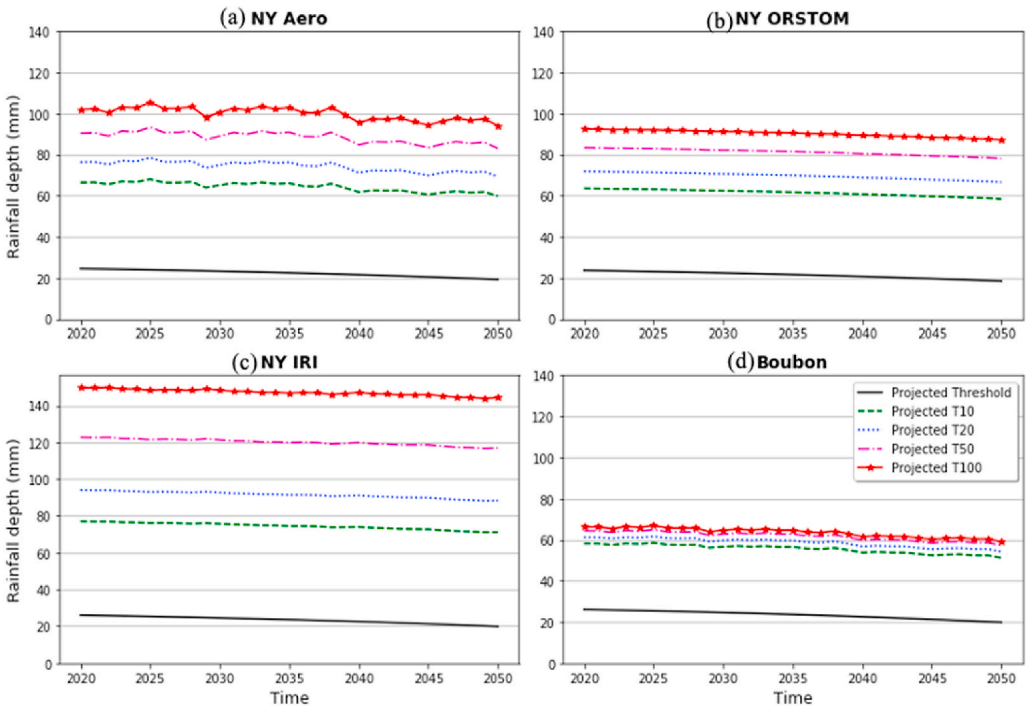

Fig. 12. Return levels of the projected extreme rainfalls at Ny-Aero (a), Ny ORSTOM (b), Ny IRI (c) and Boubon (b) stations. The legend all the graphs is in panel (d).

threshold value. This can be explained by a decrease in the extreme rainfall intensities which is supposed to vary with air temperature data. Therefore, the results showed that an increase in air temperature does not contribute to a significant increase in extreme rainfall magnitudes whereas a population increase may lead to an escalation of the number of floods.

The findings of the present paper show that extreme rainfall in the city of Niamey neither exhibit a positive trend in magnitude nor in frequency during the study period The population data used as threshold covariate in the non-stationary POT indicated that the threshold above which extreme rainfall is defined decreases over time leading to more threshold exceedances compared to the stationary POT. These findings also reveal that the increase in recent floods and rainfall related disasters are linked to a degradation of the physical conditions of urban catchments such as modifications of the soil properties (e.g., increase in soil imperviousness), settlement in flood prone areas, use of inappropriate construction materials (e.g., adobe) and insufficient drainage systems. All these factors are direct consequences of the urban population growth aggravated by a lack of urban planning strategies. Furthermore, the increase in air temperature seems to have a negligible impact on the extreme rainfall occurrence—confirming that the effect of climate change on flood occurrence seems minor compared to anthropogenic activities.

The analyses performed in this paper cover the post-1992 period for which the finest temporal resolution of rainfall record (5-min) with the fewest missing value are available for the study area. Therefore, uncertainties in the computation of the return levels greater than the sample size (24 years) may arise. Nonetheless, the extreme rainfall in the context of the study area has return levels less than one year; hence these uncertainties do not affect the characterization of extreme rainfalls developed herein.

5. Conclusions

The characteristics of extreme rainfall in the Sahelian city of Niamey were assessed under past and future climate and demographic conditions. The study begins with the selection of the most suitable temporal scale for the extreme rainfall analysis—hence enabling a better understanding of the duration and intensity of the extreme rainfall events. Although daily or seasonal rainfall data were used in past studies, it was found that the optimal temporal scale for extreme rainfall analysis in this city was 3 h, which is quite rational for a subtropical area where most of the rainfall stems from convective processes. Thus, the 3-hourly rainfall series of the considered rainfall stations for the period 1992–2015 were found to be stationary with no significant trend. Likewise, no significant trend was found in the intensities and frequencies of the extreme rainfall series constructed using stationary and non-stationary thresholds. The study further revealed that the repetitive floods and rainfall-inducing disasters observed in recent years in the city are a direct consequence of anthropogenic activities induced by a rapid population growth. Moreover, the limited drainage system adds to the daunting task of flood preparedness which in turn is increasing the vulnerability of the population. Furthermore, climate change effects, represented in this paper with air temperature data at 2 m level, seems to have less impacts on the extreme rainfall occurrence over Niamey. This result does not question the influence of climate change on the rainfall patterns over the city of Niamey and over the Sahel region in general. To do a well-founded inference on climate change influence on flood occurrence, other climate indices should be considered alongside temperature data for extreme rainfall analysis. Finally, future projections revealed that the concept of extreme rainfall in Niamey will continue to change as by the late 2040 rainfall amounts even less than 20 mm in 3 h could result disastrous for the city under the current urbanization and socio-demographic context. Therefore, adequate drainage systems and urban planning is an emergency to mitigate flood-related disasters. The concept of the extreme rainfall defined in this paper may result a useful tool for extreme rainfall analysis in all the Sahelian cities as they have similar climatic, demographic, financial and cultural characteristics.

Author contribution statement

Issa Garba: Conceived and designed the experiments; Analyzed and interpreted the data; Contributed reagents, materials, analysis tools or data; Wrote the paper.

Zakari Seybou Abdourahamane: Performed the experiments, Analyzed and interpreted the data; Contributed reagents, materials, analysis tools or data; Wrote the paper.

Funding statement

This research did not receive any specific grant from funding agencies in the public, commercial, or not-for-profit sectors.

Data availability statement

All the data used in this paper are available freely online in the cited references.

Declaration of interest's statement

The authors declare no conflict of interest.

References

[1] H. Paeth, et al., Meteorological characteristics and potential causes of the 2007 flood in sub-Saharan Africa, Int. J. Climatol. 31 (13) (2011) 1908–1926.
[2] L. Mouhamed, et al., Evolution of some observed climate extremes in the West African Sahel, Weather Clim. Extrem. 1 (2013) 19–25.
[3] P. Tamagnone, et al., Hydrology of the Sirba river: updating and analysis of discharge time series, Water 11 (1) (2019) 156.
[4] S. Sene, P. Ozer, Evolution pluviométrique et relation inondations - Événements pluvieux au Sénégal 42, 2002.
[5] F. Tazen, et al., Trends in flood events and their relationship to extreme rainfall in an urban area of Sahelian West Africa: the case study of Ouagadougou, Burkina Faso, J. Flood Risk Manag. 12 (S1) (2019), e12507.
[6] V. Aich, et al., Climate or land use?—attribution of changes in river flooding in the Sahel zone, Water 7 (6) (2015).
[7] L. Descroix, et al., Change in Sahelian Rivers hydrograph: the case of recent red floods of the Niger River in the Niamey region, Global Planet. Change 98–99 (2012) 18–30.
[8] C. Casse, M. Gosset, Analysis of hydrological changes and flood increase in Niamey based on the PERSIANN-CDR satellite rainfall estimate and hydrological simulations over the 1983–2013 period, Proc. IAHS 370 (2015) 117–123.
[9] O. Amogu, La dégradation des espaces sahéliens et ses conséquences sur l'alluvionnement du fleuve Niger moyen, in: Université Joseph Fourier : Grenoble, Université Joseph Fourier, Grenoble, 2009, p. 444.
[10] L. Descroix, et al., Spatio-temporal variability of hydrological regimes around the boundaries between Sahelian and Sudanian areas of West Africa: a synthesis, J. Hydrol. 375 (1) (2009) 90–102.
[11] L. Descroix, et al., Evolution of surface hydrology in the sahelo-sudanian strip: an updated review, Water 10 (6) (2018).
[12] H. Laurent, N. D'Amato, T. Lebel, How important is the contribution of the mesoscale convective complexes to the Sahelian rainfall? Phys. Chem. Earth 23 (5) (1998) 629–633.

[13] E.-P. Zahiri, et al., Mesoscale extreme rainfall events in west africa: the cases of Niamey (Niger) and the upper ouémé valley (Benin), Weather Clim. Extrem. 13 (2016) 15–34.
[14] B.R. Rosenzweig, et al., Pluvial flood risk and opportunities for resilience, Wiley Interdiscip. Rev. Water 5 (6) (2018) e1302.
[15] E. Kalnay, et al., The NCEP/NCAR 40-year Reanalysis project, Bull. Am. Meteorol. Soc. 77 (3) (1996) 437–472.
[16] Y. Hamere, S. Teshome, A. Mekuria, D. Ashraf, Impact of landscape pattern changes on hydrological ecosystem services in the Beressa watershed of the Blue Nile Basin in Ethiopia, Sci. Total Environ. 793 (2021), 148559, https://doi.org/10.1016/j.scitotenv.2021.148559. ISSN 0048-9697.
[17] L. Yan, et al., Nonstationary flood hazard analysis in response to climate change and population growth, Water 11 (9) (2019) 1811.
[18] INS-Niger, Tablo de Bord Social, Institut Nationale de la Statistique du Niger, Institut Nationale de la Statistique du Niger, Niamey, Niger, 2016.
[19] Weather news, Weather 72 (11) (2017) 322.
[20] S. Coles, An Introduction to Statistical Modeling of Extreme Values, in: S.S.i. Statistics (Ed.), Spring-Verlag, London, UK, 2001.
[21] A. Mailhot, et al., Regional estimates of intense rainfall based on the Peak-Over-Threshold (POT) approach, J. Hydrol. 476 (2013) 188–199.
[22] S. Begueria, et al., Assessing trends in extreme precipitation events intensity and magnitude using non-stationary peaks-over-threshold analysis: a case study in northeast Spain from 1930 to 2006, Int. J. Climatol. 31 (14) (2011) 2102–2114.
[23] J.-M. Soubeyroux, et al., Evolution des précipitations extrêmes en France en contexte de changement climatique, La Houille Blanche (1) (2015) 27–33.
[24] R. Chamani, D. Monkam, Z. Yepdo Djomou, Return times and return levels of July–September extreme rainfall over the major climatic sub-regions in Sahel, Atmos. Res. 212 (2018) 77–90.
[25] M. Roth, G. Jongbloed, T.A. Buishand, Threshold selection for regional peaks-over-threshold data, J. Appl. Stat. 43 (7) (2016) 1291–1309.
[26] C. Scarrott, A. MacDonald, A review of extreme value threshold estimation and uncertainty quantification, Rev. Statist. J. 10 (1) (2012) 33–+.
[27] Y. Tramblay, et al., Extreme value modelling of daily areal rainfall over Mediterranean catchments in a changing climate, Hydrol. Process. 26 (2012).
[28] A.N. Thiombiano, et al., Nonstationary frequency analysis of extreme daily precipitation amounts in Southeastern Canada using a peaks-over-threshold approach, Theor. Appl. Climatol. 129 (1) (2017) 413–426.
[29] J. Danielsson, et al., Using a bootstrap method to choose the sample fraction in tail index estimation, J. Multivariate Anal. 76 (2) (2001) 226–248.
[30] H.B. Issaka, D., Les inondations à Niamey, enjeux autour d'un phénomène complexe, Les. Cah. d'Outre-Mer (263) (2013) 295–310.
[31] AMMA-CATCH, AMMA-CATCH: a Hydrological, Meteorological and Ecological Observatory on West Africa, IRD, CNRS-INSU, OSUG, OMP, OREME, 1990.
[32] D. Guha-Sapir, R. Below, P. Hoyois, EM-DAT: International Disaster Database, Université Catholique de Louvain, Brussels, Belgium, 2014. www.emdat.be.
[33] INS-Niger, Institut National de la Statistique du Niger - Données Démographiques de Niamey, INS-Niger, Niamey, Niger, 2019.
[34] M.G. Kendall, Rank Correlation Methods, 4 ed., Charles Griffin, London, UK, 1975.
[35] S. Yue, et al., The influence of autocorrelation on the ability to detect trend in hydrological series, Hydrol. Process. 16 (2002) 1807–1829.
[36] Z.S. Abdourahamane, R. Acar, Analysis of meteorological drought variability in Niger and its connection with climate indices, Hydrol. Sci. J. 63 (8) (2018) 1203–1218.
[37] S.E. Said, D.A. Dickey, Testing for unit roots in autoregressive-moving average models of unknown order, Biometrika 71 (3) (1984) 599–607.
[38] W.A. Fuller, Introduction to Statistical Time Series, John Wiley and Sons, New York, 1976.
[39] R. R Core Team, A Language and Environment for Statistical Computing, R Foundation for Statistical Computing., Vienna, Austria, 2019.
[40] J.E. Heffernan, A.G. Stephenso, Ismev: an Introduction to Statistical Modeling of Extreme Values, 2018.
[41] H. Akaike, A new look at the statistical model identification, IEEE Trans. Automat. Control 19 (6) (1974) 716–723.